Photoinduced Intermolecular Electron Transfer in Micelles: Dielectric and Structural Properties of Micelle Headgroup Regions

H. L. Tavernier, Florence Laine, and M. D. Fayer*

Department of Chemistry, Stanford University, Stanford, California 94305

Received: February 19, 2001; In Final Form: June 27, 2001

Photoinduced intermolecular (donor/acceptor) electron transfer is studied both experimentally and theoretically for donors and acceptors located in the headgroup region of micelles. Fluorescence up-conversion and fluorescence yield measurements were performed to characterize photoinduced electron transfer from *N*,*N*-dimethylaniline (DMA) and *N*,*N*-dimethyl-1-naphthylamine (DMNA) to octadecylrhodamine B (ODRB) in three types of aqueous micelle solutions: dodecyl-, tetradecyl-, and cetyltrimethylammonium bromide (DTAB, TTAB, and CTAB, respectively). The data were analyzed with a detailed theory that assumes a Marcus distance-dependent rate constant. Because DMA, DMNA, and ODRB reside in the headgroup region of the micelles, the theory includes diffusion of the molecules in this region of the micelles. The micelles are modeled as a spherical core of low dielectric constant surrounded by a spherical shell headgroup region with intermediate dielectric properties, which in turn is surrounded by water. An analytical theory, which accounts for geometrical and dielectric properties of the three-region micelle environment, is used to calculate the solvent reorganization energy and free energy of transfer. To fit the data, the three-region dielectric model is necessary, and the dielectric constant of the micelle headgroup region of each micelle can be approximately determined. In addition, including local structure is required to fit the data, yielding some information about molecular organization in the headgroup region.

I. Introduction

Electron-transfer reactions have received a sustained high level of attention from the scientific community for decades due to their relevance in a wide range of applications.[1] Electron-transfer events are vital to chemical, biological, and technical processes. Numerous studies have been performed addressing the dependence of electron transfer on different environments including liquids,[2−7] micelles,[8−14] vesicles,[15] proteins,[16−19] and DNA.[20−26] Studies of electron transfer can provide information that may be useful in the design of systems for practical applications. In addition, observation of well-understood electron-transfer reactions can be used to obtain information about local environment in which electron transfer is occurring.

Electron transfer in restricted geometry systems such as micelles, reverse micelles, and vesicles attracts a great deal of interest[10−12,15,27] because of their potential to prolong the lifetime of charge-transfer states, a goal of electron-transfer studies aiming to utilize solar energy.[28−32] Micelles could be a useful medium for maintaining photoinduced charge separation because of their geometry and their multiphase character. They are composed of a hydrocarbon-like core and a headgroup region containing charged (or polar) surfactant headgroups, counterions, some water, and the first few methylene groups from the hydrocarbon tails (see Figure 1A).

Electron transfer in micelles can also provide information about the nature of the micelle environment. Because of the sensitivity of intermolecular electron transfer to many properties of local environment, it offers a unique method for probing local environments on the distance scale of angstroms. Distance distributions of molecules on these distance scales have traditionally been calculated or measured with neutron or X-ray scattering.[33] However, these experimental techniques are not sensitive to relatively low concentration solutes, so it is difficult to determine distributions involving solutes in solution. Methods are available for measurements on a larger distance scale than is probed with electron transfer. Electronic excitation transport (EET) is frequently used to probe intermolecular distances.[34−36] However, singlet EET generally occurs over tens of angstroms rather than a few angstroms.[37] Intermolecular donor−acceptor electron transfer, on the other hand, is much shorter ranged. The rate of electron transfer falls off approximately exponentially with distance on a distance scale of ∼1 Å.[38,39] Because electron transfer is a much shorter range than singlet excitation transport, it can be used to probe the headgroup region of micelles by characterizing local structure on the distance scale of individual molecules.

The time and distance dependence of electron transfer in a given system depends on properties of the donor and acceptor molecules as well as characteristics of the local environment.[8,15,20,40−45] The difference between the donor and acceptor standard potentials ($\Delta E°$), standard free energy of transfer (ΔG), and reorganization energy (λ), shown in Figure 2, determine the energetics of the reaction. These quantities are determined by solute energy levels, local dielectric properties, and molecular sizes and charges. For donors/acceptors confined to the headgroup region of a micelle, the environment cannot be approximated as a single dielectric continuum. The headgroup region has dielectric properties that are distinct from the interior of the micelle, and both the headgroup region and the interior of the micelle have dielectric properties that differ substantially from those of the bulk water, which surrounds the headgroup region. Both the reorganization energy and the free energy are modified by the micelle's "three-layer" structure, and both are

* Corresponding author. E-mail: fayer@fayerlab.stanford.edu. Fax: (650) 723−4817.

10.1021/jp0106597 CCC: $20.00
Published on Web 09/07/2001

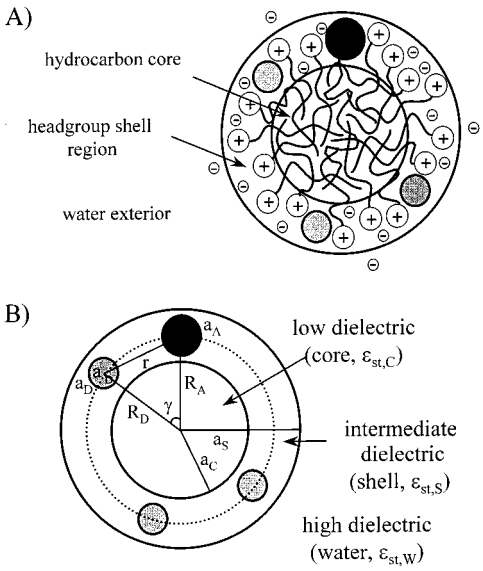

Figure 1. (A) Schematic diagram of a micelle, indicating three regions. The region inside the smaller circle contains the surfactant tails and is the hydrocarbon core. The region outside the largest circle is water with counterions. The shell between the two circles is the region of surfactant headgroups (+), most of the counterions (−), the donor (black) and acceptor molecules (shaded), portions of the surfactants' hydrocarbon tails, and some water. The dielectric properties of this region are intermediate between those of water and hydrocarbon. (B) Model for electron transfer in the headgroup region of a micelle, incorporating a three-region dielectric structure. The donor and acceptor spheres, with radii $a_{D/A}$, lie at distances $R_{D/A}$ from the center of the micelle and diffuse on spherical surfaces with radii $R_{D/A}$. r is the distance between the donor and an acceptor. γ is the angle between the lines joining the center of the micelle with the centers of a donor and an acceptor pair. The interior of the micelle is taken to be a sphere of radius a_C with a low static dielectric constant. Donor and acceptor spheres are located outside the micelle core in a shell of radius a_S that surrounds the micelle core. Finally, the shell is surrounded by water.

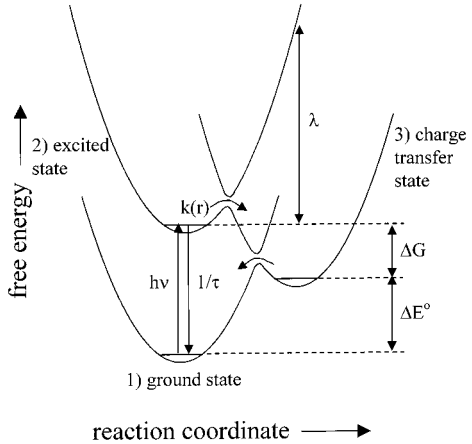

Figure 2. Free energy diagram of three-state model consisting of (1) donor and acceptor ground state, (2) photoexcited donor and ground-state acceptor (or photoexcited acceptor and ground state donor), and (3) charge-transfer state. Excited-state population is created by photoexcitation with energy $h\nu$ and removed by relaxation to the ground state with fluorescence lifetime τ and electron transfer with rate $k(r)$. The free energy difference between ground and charge-transfer states is the difference between donor and acceptor redox potentials, $\Delta E° > 0$. The free energy difference between excited and charge-transfer states is $\Delta G < 0$, the standard free energy associated with electron transfer. λ is the reorganization energy. Molecules, which undergo electron transfer, return to the ground state via geminate recombination.

sensitive to the properties of each layer. In addition, individual donor and acceptor molecular properties determine the magnitude and distance dependence of their electronic coupling. It has been shown for different solvents and different donor−acceptor systems that intermolecular electron-transfer data are not properly described by a contact-only or Collins-Kimball rate.[2,4,46,47] It is necessary to include the distance dependence of the electronic coupling in the distance-dependent rate constant. The Marcus rate depends on the magnitude and distance dependence of donor−acceptor orbital overlap. In addition, the Marcus theory includes the distance-dependent free energy change of transfer and the distance-dependent reorganization energy (ΔG and λ in Figure 2). The resulting rate constant can have strong distance dependence. Because of the effects of local structure on ΔG and λ, the magnitude and distance dependence of the electron-transfer rate in heterogeneous environments can also be very different from a simple continuum rate constant.[20,8]

In donor/acceptor (nonbridged) intermolecular electron transfer, diffusion and solvent-influenced donor−acceptor distance distributions play an important role in determining the time dependence of electron transfer and, therefore, experimental electron-transfer observables.[46,48−51] The donor−acceptor distance distribution is included in the electron-transfer theory through a radial distribution function, $g(r)$, which determines the effective acceptor concentration participating in the reaction at a given distance. $g(r)$ is determined by local molecular structure and can cause notable deviations from the bulk acceptor concentration at short donor−acceptor distances. The rate of diffusion is distance-dependent as described by the hydrodynamic effect.[52−54] The distance dependence of diffusion is brought into the electron transfer theory through $D(r)$, the distance-dependent diffusion parameter.[51] The consequence of the hydrodynamic effect is slower diffusion at short donor−acceptor distances. The hydrodynamic effect can slow diffusion near contact by a factor of 4 compared to bulk diffusion.[52,53] Because most electron transfer occurs near contact, the radial distribution function and the hydrodynamic effect can have a significant influence on the time dependence of intermolecular electron transfer in a given system.[2,3,5,51]

In this paper, experimental data are presented for electron transfer between octadecylrhodamine B (ODRB) and either *N*,*N*-dimethylaniline (DMA) or *N*,*N*-dimethyl-1-naphthylamine (DMNA) in three types of aqueous micelle solutions: dodecyl-, tetradecyl-, and cetyltrimethylammonium bromide (DTAB, TTAB, and CTAB, respectively). The donor and acceptor molecules are located in the headgroup regions of the micelles. The data were analyzed with a statistical mechanical theory that encompasses a number of key elements that affect photoinduced intermolecular electron transfer as discussed above.[49,51,55,56] The theory, which incorporates a distance-dependent rate constant, solvent structure, and diffusion of the donor and acceptors in the headgroup regions of the spherical micelles, can be used to calculate electron-transfer observables. A Marcus distance-dependent transfer rate was used to describe through-solvent transfer and incorporates solvent dielectric constants, redox potentials, excitation energies, and Coulomb interactions. λ and ΔG were calculated for a three-region dielectric model of the micelle. Local molecular structure is included as a model for the donor−acceptor distance distribution at the micelle surface and the hydrodynamic effect is included in the form of a distance-dependent diffusion constant. All parameters necessary for the data analysis are measured, calculated, or known with the exception of the donor−acceptor electronic coupling parameters and micelle headgroup region properties. The theory is able to reproduce both the functional form of the time

dependence and the concentration dependence of the data. The data cannot be fit without the three-region micelle model. The dielectric constant of the micelle headgroup region can be inferred from fits to the data. In addition, it is not possible to fit the data without including a donor−acceptor distance distribution determined by local structure. As a result, fits to the data yield some information about molecular organization in the headgroup region. Excellent fits to the DMA/ODRB/CTAB data were obtained with the same electronic coupling parameters determined for electron transfer between DMA and rhodamine 3B (R3B, ODRB with a 2-carbon rather than a 18-carbon tail) in a number of liquids.[2,3] The information about the headgroup region of the CTAB micelles derived from these fits was used to determine the electronic coupling for DMNA/ODRB in CTAB. These electronic coupling parameters, in turn, were used to determine headgroup region properties of TTAB and DTAB micelles. The results show that the theory, including a distance-dependent transfer rate, diffusion on the micelle surface, and λ and ΔG for the three-region model, does a respectable job of accounting for the intricacies of interaction between donor, acceptor, and micelle in electron transfer.

II. Model and Theory

A. The Model. In the experiments, micelles were chosen that are spherical and monodispersed.[9,57,58] The micelles were modeled as three-region systems (see Figure 1B). The core of a micelle, which contains the hydrocarbon tails of the surfactant molecules, has approximately the density of pure hydrocarbon.[59,60] It is modeled as a sphere of radius a_C and given the dielectric properties of a hydrocarbon. Surrounding the core is a spherical shell, which contains the donor and acceptor molecules, surfactant headgroups and counterions, some water, and some methylene units from surfactant tails. Headgroup and counterion charges are neglected, and the region is given dielectric properties somewhere between hydrocarbon and water. Finally, these two regions are surrounded by water. While the model is an approximate representation of the problem of electron transfer in micelles, it is sufficiently detailed to illustrate the importance of factors that are prominent in other contexts such as electron transfer between donors and acceptors in liquid solution.[5,8,40−42]

There is at most one donor molecule per micelle, but there can be many acceptors. In this paper, ODRB is referred to as the "donor" molecule even though it is a hole donor rather than an electron donor. This terminology has been chosen to be consistent with the notation in the previously developed theory.[2,4,8,61,62] In the theory and in this experiment, the "donor" is the molecule that is in low concentration and is photoexcited. Accordingly, DMA and DMNA are referred to as the hole "acceptors". The donor and acceptor molecules were chosen so that they reside in the headgroup region of the micelles (see Figure 1A). (A fraction of the acceptors do not bind to the micelle and are in the water. These acceptors do not participate in the electron transfer. The fraction of acceptors in the micelles is determined experimentally for each micelle. See below.)

The donor and acceptor molecules are modeled as spheres with radii a_D and a_A, respectively. They reside at distances R_D and R_A from the center of the micelle and diffuse in the headgroup region, modeled as a spherical shell, at the appropriate distance from the center of the micelle (see Figure 1B). Although λ and ΔG can be calculated for $R_D \neq R_A$, the diffusion problem is only tractable if both donors and acceptors diffuse with their centers equidistant from the center of the micelle. Therefore, the centers of the donor and acceptor spheres are taken to be at distance $R = R_D = R_A$ from the center of the supporting sphere, as shown in Figure 1B. For this case, their center-to-center separation distance can be characterized uniquely by either r or γ (see Figure 1B), where γ is the angle between the lines joining the centers of the donor and acceptor molecules to the micelle center. The donor−acceptor separation distance is

$$r = 2R \sin(\gamma/2) \tag{1}$$

and the contact distance is $r_m = 2R \sin(\gamma_m/2)$. γ_m is the angle at which the donor and acceptor hard spheres are in contact. In the analysis of the distance dependence of the transfer rate, R is taken to be a constant, determined by the micelle size. The headgroup shell has an inner diameter of a_C and an outer diameter of a_S. The theory has the donor and acceptors completely contained within the headgroup shell, so that $a_C \leq R - \max(a_D, a_A)$ and $a_S \geq a_C + 2\max(a_D, a_A)$.

There is at most one donor molecule per micelle, and the micelles are in low enough concentration that donors are noninteracting. Therefore, the theory uses a model in which a micelle contains a single donor molecule and a given number of acceptor molecules, all diffusing in the micelle headgroup region. The donor can transfer a hole (electron) to any one of a number of ground-state acceptors on the same micelle.

Photoinduced electron transfer can be modeled by a three-state system. Figure 2 is a free energy diagram of a three-state electron-transfer system representing transfer in the normal, noninverted regime. The lowest parabola represents the initial system, with all molecules in their respective ground states. Photoexcitation of the donor brings the system into the state represented by the highest parabola. Following photoexcitation, the system either relaxes to the ground state or progresses to the charge-transfer state by transferring an electron with the distance-dependent transfer rate, $k(r)$. Molecules that undergo electron transfer can return to the ground state via geminate recombination.

The foundation of the data analysis used in this work is a statistical mechanical theory that averages over all donor positions to determine the time-dependent excited-state survival probability $\langle P_{ex}(t)\rangle$ (probability that the photoexcited molecule is still excited at time t after excitation), which is represented by the experimentally observed time-dependent fluorescence. Fluorescence yield can be determined by taking the area under the time-dependent calculation. Together, the distance-dependent rate constant and donor−acceptor distances at a given time determine the survival time of the excited state.

B. Electron-Transfer Rate Constant. For electron transfer in the normal region ($-\Delta G < \lambda$), a widely used form of $k(r)$ for nonadiabatic transfer was developed by Marcus:[38,40,41,63−65]

$$k(r) = \frac{2\pi}{\hbar} J_o^{\,2} \exp[-\beta(r - r_m)] \frac{1}{\sqrt{4\pi\lambda k_B T}} \exp\left[\frac{-(\Delta G + \lambda)^2}{4\lambda k_B T}\right] \tag{2}$$

where r is the donor−acceptor center-to-center distance, r_m is the donor−acceptor contact distance (the sum of the donor and acceptor hard sphere radii), $2\pi\hbar$ is Planck's constant, k_B is Boltzmann's constant, and T is temperature. The donor−acceptor electronic coupling is characterized by J_o, the magnitude of coupling at contact, and β, which reflects the exponential distance dependence of the coupling. $\lambda(r)$ is the solvent reorganization energy, and $\Delta G(r)$ is the standard free energy

change of transfer. The donor−acceptor distance is the through-sphere distance, $r = 2R \sin(\gamma/2)$, shown in Figure 1B. In some situations, electron transfer can be adiabatic.[66,67] For previous experiments in liquids involving the most strongly coupled donor−acceptor pair used in this study, it was not possible to fit the data with an adiabatic transfer rate.[3] Therefore, only the Marcus nonadiabatic transfer rate will be used.

The Marcus form of λ for spherical reagents in a dielectric continuum[40,41,63,64] and the Rehm−Weller form of ΔG for similar conditions[42] are not directly applicable to the problem of electron transfer in the headgroup region of a micelle because of the heterogeneous nature of the dielectric environment.[8,20] The same approaches to calculating λ and ΔG can be used for heterogeneous environments if all space except the donor and acceptor volume is divided into regions with distinct dielectric properties,[8,20] as in the three-region micelle model described at the beginning of this section. An analytical theory for calculating λ and ΔG in a micelle environment has been presented elsewhere and will be summarized in the following sections.[8,68]

1. Solvent Reorganization Energy (λ) in Heterogeneous Systems. The reorganization energy, λ, shown in Figure 2, is the free energy change that would be required to reorient atoms and molecules as if they were forming and solvating the product state but without actually transferring an electron. λ includes an inner sphere portion, λ_i, and an outer sphere portion, λ_o:[64]

$$\lambda = \lambda_i + \lambda_o \tag{3}$$

where λ_i describes intramolecular structural changes associated with removal of an electron from the donor and addition of an electron from the acceptor and λ_o describes solvent reorganization about the products. The inner-sphere reorganization energy can be calculated from the change in bond length and the force constants of the normal modes of the molecules.[64] According to Marcus, the outer sphere (solvent) reorganization energy depends on the size of reactants and the separation distance, as well as on the dielectric properties of the surrounding solvent.[40,41,63,64] In his original formulation, a homogeneous, continuum solvent was considered.

The continuum approach can be extended to heterogeneous media if all space can be divided up into a number of regions with different dielectric properties.[8,68] For the three-region micelle model, λ_o can be written as follows:

$$\lambda_o = \frac{e^2\alpha_S}{32\pi^2\epsilon_o}\int_{v_\infty - v_D - v_A}(\mathbf{E}_D - \mathbf{E}_A)^2\,dV + \frac{e^2(\alpha_C - \alpha_S)}{32\pi^2\epsilon_o} \times \int_{v_C}(\mathbf{E}_D - \mathbf{E}_A)^2\,dV + \frac{e^2(\alpha_W - \alpha_S)}{32\pi^2\epsilon_o}\int_{v_W}(\mathbf{E}_D - \mathbf{E}_A)^2\,dV \tag{4}$$

where S represents the headgroup shell region in which the donor and acceptor reside, C represents the micelle core, and W represents the surrounding water. $\alpha_q = \epsilon_{op,q}^{-1} - \epsilon_{st,q}^{-1}$, $\epsilon_{op,q}$, and $\epsilon_{st,q}$ denote the optical and static dielectric constants of the appropriate region, v_qs denote the volumes of the appropriate micelle regions or donor/acceptor spheres, e is the charge of an electron, and ϵ_o is the permittivity of free space. $\mathbf{E}_{D/A}(\mathbf{r}) = -\nabla|\mathbf{r} - \mathbf{r}_{D/A}|^{-1}$ is the electric field at point $\mathbf{r}$ associated with charged donor/acceptor conducting spheres located at $\mathbf{r}_{D/A}$, in a vacuum. The first term in this equation integrates over all space except donor and acceptor volumes and represents the solvent reorganization energy in a solvent continuum with the dielectric properties of the shell. The second term includes the contribution from the micelle core, minus the contribution of the shell over that region. Similarly, the third term is the contribution from the surrounding water, minus the contribution from the shell dielectric over that region. Analytical solutions to the integrals have been presented previously[8,68] and can be found in Appendix A. The Marcus expression for λ_o in a continuum solvent can be obtained by taking the first term in eq 4 and removing the Kharkats corrections[69] for donor and acceptor volumes.

The model neglects all the charges except those participating in the electron-transfer event, even though the micelle system consists of many charged headgroups with counterions. However, it has been discussed in the literature that the effect of small ionic species should be modest compared with the orientational reorganization energy of polar solvent molecules.[70]

2. Free Energy of Transfer (ΔG) in Heterogeneous Systems. $\Delta G(r)$, shown in Figure 2, is the standard free energy change associated with photoinduced electron transfer. It is another distance-dependent parameter that affects the distance-dependent electron-transfer rate constant. Determination of $\Delta G(r)$ requires knowledge of redox potentials of the donor and acceptor and calculation of the distance-dependent Coulombic interactions of the reactants and products. Often, redox potentials are known for donor and acceptor molecules in a bulk liquid but not in the heterogeneous dielectric environment of an experiment. The different local dielectric environments near the donor and acceptor molecules also affect Coulombic interactions. However, these factors can be calculated to determine the distance dependence of ΔG in heterogeneous systems.[8,20]

The free energy change of photoinduced electron transfer can be written:[71]

$$\Delta G(r) = IP_D - EA_A - W_r + W_p - h\nu \tag{5}$$

where IP_D is the ionization potential of the donor, EA_A is the electron affinity of the acceptor, $W_{r/p}$ denotes the total energy change to bring the reactants/products together in the dielectric environment of interest at the given separation distance, and $h\nu$ is the donor singlet excited-state energy, taken to be the energy at which donor's normalized absorption and fluorescence spectra cross.[65]

Weller calculated ΔG in a bulk solvent with a known static dielectric constant when redox potentials are known in a solvent with a different static dielectric constant.[72] Following his method, ΔG in a heterogeneous system can be calculated from redox potentials measured in bulk solution. The difference between IP_D and EA_A can be written in terms of donor and acceptor redox potentials ($E_{D/A}^{ox/red}$) and solvation free energies as follows:

$$IP_D - EA_A = (E_D^{ox} - E_A^{red})_B + \left(1 - \frac{1}{\epsilon_{st,B}}\right)(S_p - S_r) \tag{6}$$

where B denotes measurements made in a bulk liquid with static dielectric constant $\epsilon_{st,B}$. The redox term for bulk solution can be measured experimentally with cyclic voltammetry. $S_{r/p}$ is the solvation energy of individual reactant or product ions in a vacuum:

$$S_{r/p} = \frac{e^2}{32\pi^2\epsilon_o}(q_D^2\int_{\infty - v_D}E_D^2\,dV + q_A^2\int_{\infty - v_A}\mathbf{E}_A^2\,dV) = \frac{e^2}{8\pi\epsilon_o}\left(\frac{q_D^2}{a_D} + \frac{q_A^2}{a_A}\right) \tag{7}$$

where q_D and q_A are the charges on the donor and acceptor in units of e. Reactant charges are used for calculation of S_r and product charges for S_p. Solvation energies calculated in this section assume a reference state of infinitely separated reactants/products in a vacuum. Because $IP_D - EA_A$ is a relation of gas-phase properties, eq 6 applies to both micelle and bulk liquid systems.

$W_{r/p}$ terms incorporate both solvation energies and Coulomb interactions of the ions. For the three-region micelle model they can be written as

$$W_{r/p} = \frac{e^2}{32\pi^2\epsilon_o}\left[\frac{1}{\epsilon_{st,S}}\int_{\infty-\upsilon_A-\upsilon_D} + \left(\frac{1}{\epsilon_{st,C}} - \frac{1}{\epsilon_{st,S}}\right)\int_{\upsilon_C} + \left(\frac{1}{\epsilon_{st,W}} - \frac{1}{\epsilon_{st,S}}\right)\int_{\infty-\upsilon_S-\upsilon_C}\right](q_D\mathbf{E}_D + q_A\mathbf{E}_A)^2\,dV - S_{r/p} \quad (8)$$

Reactant and product charges are used for W_r and W_p, respectively.

The expression for ΔG in a continuum can be obtained when eqs 5−7 are used with the first term in eq 8, with $\epsilon_{st,S} = \epsilon_{st}$. If the Kharkats corrections for donor and acceptor volume are neglected in this expression, the Rehm−Weller expression[42] for a continuum is obtained.

If the donor and acceptor are in the same dielectric region, these expressions for ΔG and λ can be rewritten for any heterogeneous dielectric environment in which all space is divided into regions and each region can be described with specific optical and static dielectric constants.[20] Appendix A contains analytical solutions to the integrals in eqs 4 and 8 for the micelle three-region dielectric model.[8] Properly modeling the heterogeneous dielectric nature of the micelle system can lead to very different calculated rate constants compared to a continuum approach (see Appendix B) and can have a significant impact on the results of data analysis.[8,20]

C. Experimental Observables. In the experiments presented in this work, electron transfer is induced by photoexcitation of a donor molecule. The donor is photoexcited and undergoes relaxation to the ground state (fluorescence and nonradiative decay) or electron transfer to any of the acceptors on the same micelle. Transfer results in quenching of the donor fluorescence. The experimental observables that are modeled theoretically are time-dependent and steady-state donor fluorescence. Transient absorption measurements could also be made to measure the time-dependent excited-state population. The time dependence of acceptor fluorescence or the excited-state transient absorption is an observable that corresponds to the ensemble averaged excited-state survival probability as a function of time, $\langle P_{ex}(t)\rangle$. Details of the theory for micelles have been presented elsewhere without a distance-dependent diffusion constant and without the effect of solvent structure.[61,62] The results will be summarized here with these two important effects added.

Diffusion and the rate of forward transfer can be accounted for theoretically starting with the one-donor, one-acceptor case. $S_{ex}(t|\gamma_o)$ is the probability that the donor is still excited at time t, given that it was photoexcited at $t = 0$ and that the donor and acceptor were separated by angle γ_o (distance r) at that time, for the one-donor, one-acceptor case. All distances are center-to-center distances. $S_{ex}(t|\gamma_o)$ is the solution the following differential equation, with initial and reflecting boundary conditions as follows:[61,62]

$$\frac{\partial}{\partial t}S_{ex}(t|\gamma_o) = L_{\gamma_o}{}^{+}S_{ex}(t|\gamma_o) - k(\gamma_o)S_{ex}(t|\gamma_o)$$

$$S_{ex}(0|\gamma_o) = 1$$

$$\frac{\partial}{\partial\gamma_o}S_{ex}(t|\gamma_o)|_{\gamma_o=\gamma_m} = 0 \quad (9)$$

where t is time and γ_o is the initial angular position of the acceptor with respect to the donor, written in terms of angle (see Figure 1B). $k(\gamma_o)$ is the rate constant of electron transfer at that distance. The donor and acceptor molecules cannot approach closer than the sum of their hard sphere radii, which is represented angularly by γ_m. $L_{\gamma_o}{}^{+}$ is the adjoint of the Smoluchowski diffusion operator:

$$L_{\gamma_o}{}^{+} = \frac{1}{R\sin\gamma_o}\exp\left(\frac{V(\gamma_o)}{k_BT}\right)\frac{\partial}{\partial\gamma_o}D(\gamma_o)\frac{\sin\gamma_o}{R}\times \exp\left(-\frac{V(\gamma_o)}{k_BT}\right)\frac{\partial}{\partial\gamma_o} \quad (10)$$

where R is the radius of the sphere on which the donor and acceptor diffuse, $D(\gamma_o)$ is the distance-dependent lateral diffusion coefficient, k_B is Boltzmann's constant, T is temperature, and $V(\gamma_o)$ is the distance-dependent potential in which the acceptors are diffusing. Note that the donor−acceptor separation distance is completely defined by γ, so the diffusion is one-dimensional. Equation 9 for $S_{ex}(t|\gamma)$ cannot be solved analytically, and numerical evaluation must be followed by numerical integration.

The experimentally observed ensemble averaged excited-state survival probability in a micelle with one donor and n acceptors is

$$\langle P_{ex}(t)\rangle_n = e^{-t/\tau}\left[\int_{\gamma_m}^{\pi} S_{ex}(t|\gamma_o)2\pi R^2\sin\gamma_o g(\gamma_o)\,d\gamma_o\right]^n \quad (11)$$

where τ is the fluorescence lifetime of the donor in the absence of electron transfer. $g(\gamma)$ is the solvent radial distribution function used to model the donor−acceptor distance distribution. To get the final experimentally observable quantity, eq 11 must be combined with the fact that acceptor molecules are not distributed uniformly among micelles.

Acceptor molecules are assumed to follow a Poisson distribution about N, the mean number of micelle-bound acceptors per micelle. Then, the observable, $\langle P_{ex}(t)\rangle$, is

$$\langle P_{ex}(t)\rangle = \sum_{n=0}^{\infty}\frac{e^{-N}N^n}{n!}\langle P_{ex}(t)\rangle_n \quad (12)$$

$\langle P_{ex}(t)\rangle$ is independent of donor concentration because it applies to the case in which donor concentration is low enough that each micelle has at most one donor.

In addition to measuring and calculating the time-dependent fluorescence, it is valuable to study the steady-state fluorescence yield, Φ. In the time-dependent measurements presented below, the shortest time scale behavior of the electron transfer is masked by the convolution of the instrument response with the electron-transfer dynamics. Fluorescence yield experiments are sensitive to the integrated area of the unconvolved $\langle P_{ex}(t)\rangle$. As a result, they provide information about electron-transfer dynamics that are obscured by instrument response in the time decays. Because the fluorescence yield is not limited by the time resolution of the time-dependent experiments, it provides some information about electron-transfer dynamics on the time scale shorter than the laser pulse length. Φ is the ratio of steady-state fluorescence from a sample with acceptors to one with no acceptors. It can

be written using the integrated areas under unconvolved $\langle P_{ex}(t)\rangle$ curves:

$$\Phi = \frac{\int_0^\infty \langle P_{ex}(t)\rangle \, dt}{\tau} \tag{13}$$

where the area under $\langle P_{ex}(t)\rangle$ with no acceptors is the fluorescence lifetime, τ. In fitting data, the fluorescence time decays and fluorescence yield experiments are fit simultaneously.

D. Solvent Structure and the Hydrodynamic Effect. In the theoretical description of electron transfer in liquids,[51] the effects of solvent structure on solute−solute distance distributions and the hydrodynamic effect[52−54,73,74] were included based on the vast amount of information available in the literature. It was found that a hard-sphere solvent radial distribution function, $g(r)$, was adequate for describing the solute−solute distance distribution in the calculations.[5] In addition, analytical forms for the hydrodynamic effect, $D(r)$, are available for liquids.[52,53,74] However, no equivalent treatments for either $g(r)$ or $D(r)$ exist for the headgroup regions of micelles. As in the experiments on liquids,[2−5] it was found that agreement between theory and experiment could not be achieved for the electron-transfer experiments in micelles without the inclusion of $g(r)$. As an approximation, the three-dimensional forms of $g(r)$ and $D(r)$ have been employed. As shown below in the data analysis, the 3D forms appear to work well.

$g(r)$ is used to describe the distribution of acceptor molecules about the donor molecules.[75] For hard-sphere solute/solvent molecules with low solute concentrations (less than a few tenths molar), solute molecules tend to follow the structure determined by the solvent molecules.[75] This means that acceptor molecules follow the solvent radial distribution function about a donor molecule. The peak in $g(r)$ in the first solvent shell and the oscillatory nature of $g(r)$ have profound effects on the probability of finding an acceptor near a donor. Because electron transfer is short range, these short-range oscillations have a strong influence on the time dependence of electron transfer.

For this work, hard-sphere radial distribution functions are calculated by solving the Percus−Yevick equation,[75−79] using an algorithm given by Smith and Henderson[80] and modified by a Verlet−Weis correction.[81] r is the donor−acceptor center-to-center separation distance, so all radial distribution functions are shifted so that the first peak is at the sum of donor and acceptor radii. Dense, room-temperature liquids generally have a range of packing fractions $\eta = 43-48\%$.[75,81−84] Therefore, $\eta = 45\%$ was used in the calculations.

Diffusion is affected by $g(r)$ because the nature of the diffusion must preserve $g(r)$. Diffusion that maintains $g(r)$ can be included in the theory by requiring the diffusion to occur within a potential of mean force:[33,54,74]

$$w(r) = -k_B T \ln[g(r)] \tag{14}$$

If both of the reactants have nonzero charges, the Coulomb interaction also affects diffusion. The total potential in which the donor and acceptor molecules diffuse can be written:

$$V(r) = w(r) + \frac{q_{Dr} q_{Ar} e^2}{4\pi\epsilon_o \epsilon_{st} r} \tag{15}$$

where ϵ_{st} is the static dielectric constant of the continuum solvent. $V(r)$ can be included in eq 10 for diffusion in three dimensions. $V(r)$ including a Coulomb potential can be calculated for a heterogeneous medium in the same way that ΔG was calculated above and included in eq 10 for diffusion in the micelle headgroup region.

A distance-dependent diffusion constant, $D(r)$, accounts for the hydrodynamic effect, in which molecules diffuse toward each other slower at short distances because solvent molecules entrained to move in the direction of a diffusing solute molecule repel other nearby solute molecules.[52−54,73,74] $D(r)$ can be expressed theoretically with forms that depend on whether stick or slip boundary conditions are appropriate for the particular experimental system. An expression for $D(r)$ was developed by Deutsch and Felderhof[52,53] for the case of stick boundary conditions, which are most appropriate when solute molecules are larger than the solvent molecules.[54] An expression for $D(r)$ using slip boundary conditions, which are most appropriate when solute and solvent molecules are similar sizes,[54] has been developed by Northrup and Hynes:[74]

$$D(r) = D\left[1 - \frac{1}{2}\exp\left(\frac{r_m - r}{\sigma}\right)\right] \tag{16}$$

where D is the sum of the donor and acceptor bulk diffusion coefficients, r_m is the donor−acceptor contact distance, and σ is the solvent diameter.

The influence of $g(r)$ and $D(r)$ on electron transfer has been illustrated previously for liquid solutions.[2,3,5,51] Compared to calculations that omitted $g(r)$ and $D(r)$, the electron-transfer dynamics are modified significantly. The changes brought about by the inclusion of $g(r)$ and $D(r)$ are of similar nature in micelles to those illustrated for liquids. The details of the influence of $g(r)$ and $D(r)$ on electron-transfer dynamics in a specific system depend on the exact parameters of that system. However, some general statements can be made. Compared to calculations that omit $g(r)$ and $D(r)$, $g(r)$ influences the short time behavior and $D(r)$ influences the longer time behavior. $g(r)$ increases the local concentration of acceptors that are very close to the donor, making the short time transfer faster than it would be in an isotropic continuum. $D(r)$ slows the approach of donor and acceptor by diffusion, which slows the longer time transfer. It will be shown that $D(r)$ does not have a discernible effect for the experimental circumstances of electron transfer contained in this paper. However, $D(r)$ must be included when analyzing a new set of experimental data, because it is difficult to predict whether $D(r)$ will have an effect for a given set of conditions.

The electron-transfer observable, the donor excited state population, has a complex, nonexponential time-dependence that can only be properly described when the ensemble averages over distances are properly performed by using a distance dependent transfer rate, $g(r)$ and $D(r)$.

III. Experimental Procedures

Details of the sample preparation have been presented elsewhere.[9] The only difference is that two "hole" acceptors, DMNA and DMA, are studied. In short, three types of micelles, DTAB, TTAB, and CTAB, are used to make aqueous solutions with surfactant concentrations just above their respective critical micelle concentrations, which ensures that the micelles formed are spherical and monodispersed.[9,57,58] DTAB and TTAB were the highest commercial grade available from Aldrich, and CTAB was obtained from Fluka (99+%). Micelle concentrations were 206 μm for all micelle systems. Critical micelle concentration, cmc, and aggregation number, N_{agg}, are reported in Table 1.

ODRB, the photoexcited hole donor, was obtained from Molecular Probes. The ODRB molecules are tethered into the

TABLE 1: Micelle Characteristics

micelle	cmc, mM[121]	N_{agg}[121]	*R*, Å
DTAB	15.0	50	16.7
TTAB	3.5	67	19.2
CTAB	0.8	92	21.7

micelles by their 18-carbon chains, with the charged rhodamine portion of the molecules in the headgroup region.[35] Octadecylrhodamine B is not a zwitterion like rhodamine B. ODRB is the octadecyl ester of rhodamine B. The ester replaces the carboxylic acid of rhodamine B. The concentration of ODRB is 20 μM, whereas the micelle concentration is 206 μM. This ensures that there is at most one ODRB per micelle. ODRB has a negligible affinity for the aqueous phase but exists bound to the micelle. Fluorescence anisotropy studies of electronic excitation transfer among ODRB molecules in micelles have shown that the chromophore headgroups of ODRB are located at the micelle surface in the micelle headgroup region.[35] This is consistent with what would be expected for a molecule comprised of a long hydrocarbon chain attached to a charged group.

DMA and DMNA were the highest quality available from Aldrich and used without further purification. DMA was purchased sealed under nitrogen. For each of the micelle/donor combinations, four samples were prepared: one sample was made with only ODRB, and three samples were made with ODRB and different DMA/DMNA concentrations. Because time-dependent and fluorescence yield measurements were performed at different times, two entire sets of samples were prepared so that both measurements could be made with fresh samples. DMA as the acceptor was studied in CTAB only. DMNA was studied in CTAB, TTAB, and DTAB. Data taken on the DMA/ODRB samples in all three micelles have been presented previously.[8,9] However, it was assumed in the previous studies that 100% of the DMA put into solution was bound to the micelles. In the current study, it was determined that a substantial fraction of the DMA remains in the water and does not participate in electron transfer. Close to 100% of DMNA binds to the micelles. As discussed below, the fraction bound to each micelle was determined. Because the binding of DMNA to the micelles is almost complete, error in the determination of the fraction that remains in the water is smaller for DMNA than for DMA. The DMAs are more strongly bound to CTAB as compared to the smaller micelles.

DMA has been shown to reside near the surface of micelles.[85] NMR measurements in CTAB solutions showed a large shift of N−CH and α-CH protons upon addition of even small amounts of DMA. Such a shift is consistent with localization of an aromatic ring near these protons. Chemical shifts on protons associated with methylene groups farther from the surface occur only at DMA concentrations >0.7 times the CTAB concentration, when the deeper hydrocarbon protons near the micelle interior begin to show substantial shift. This is interpreted as due to penetration of DMA into the micelle occurring at very high DMA concentrations after saturation of the surface region.[85] Furthermore, at such high doping levels, the structure of micelles changes substantially.[86−89] There is a large increase in the aggregation number, and there can be shape changes. Therefore, the location of DMA at high doping concentration does not provide information on the situation encountered in the current experiments. For the concentrations used in this paper, the NMR study indicates that DMA molecules will be in the headgroup region rather than in the interior of the micelles. It is expected that DMNA will behave similarly to DMA and be located in the headgroup region.

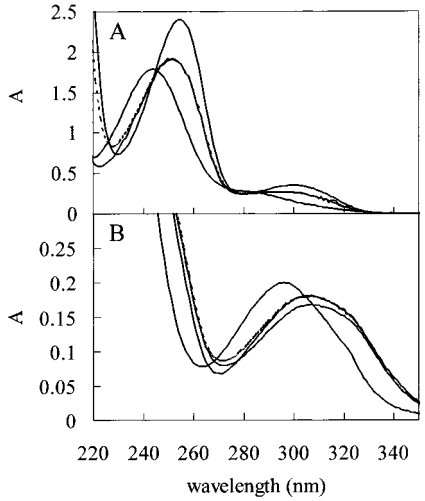

Figure 3. Absorption spectra of DMA (A) and DMNA (B) in aqueous CTAB solutions. From left to right, solid curves are spectra taken with sub-cmc surfactant (no substrate bound to micelles), experimental surfactant concentration ([M] = 206 μm), and 10 times experimental surfactant concentration (essentially all substrate bound to micelles). All curves shown in each figure represent the same substrate concentration. The dashed line represents a superposition of *x* times the unbound spectrum and (1 − *x*) times the bound spectrum, where 100*x* is the percent of substrate bound to the micelle in the experimental solutions. For DMA/CTAB, % bound = 58. For DMNA/CTAB, % bound = 94.

A study using neutron scattering determined the penetration of water into CTAB, TTAB, and DTAB.[90] The study showed that water is found some distance into the headgroup region, but not in the cores. In CTAB and TTAB, water is present as far as ∼2.5 methylenes into the micelles, while it penetrates up to ∼4 methylenes in DTAB. The part of the micelles composed of the actual headgroups and the methylenes that are exposed to water comprise the headgroup region of the micelles. DMA and DMNA are both polar and polarizable. DMA is mildly soluble in water, and DMNA is slightly soluble in water (see below). The mixed water/hydrocarbon headgroup region of the micelles is a good solvent for both DMA and DMNA relative to the pure hydrocarbon micelle cores. A recent study of the location of 2-ethylnaphthalene (2EN) in micelles[91] showed, for example, that ∼80% of 2EN is located in the headgroup region of TTAB and ∼20% is in the core. Both DMA and DMNA are substantially more polar than 2EN, which should shift their distributions to the headgroup region.

Further evidence for the location of DMA and DMNA was obtained by using fluorescence spectroscopy. While the absorption spectra change with the medium to some extent (see Figure 3), the fluorescence spectra show a dramatic shift. For example, the peaks of the fluorescence spectra of DMNA in hexane, CTAB, TTAB, DTAB, and water are located at 379, 429, 431, 433, and 447 nm, respectively. The peak positions in the micelles are significantly different from those in either pure water or pure hydrocarbon. Therefore, the DMNA is located in an environment that is intermediate between water and hydrocarbon, consistent with the headgroup region. Based on the fluorescence spectra, assignment of the location of the chromophores to the headgroup region is consistent with the neutron scattering data that show there is significant water, in addition to methylenes, present in the headgroup regions of the micelles.

Several methods have been presented for determining the binding constant of substrate molecules to micelles.[92,93] Using the same principles as in these methods, binding constants were determined for the four micelle systems presented in this paper. UV−vis spectra were obtained for both DMA and DMNA in

TABLE 2: Substrate Concentrations in the Four Micelle Systems

substrate	micelle	N up-conversion[a]	N yield[a]	% bound
DMA	CTAB	5.9, 8.4, 12.5, 16.6	5.3, 7.5, 10.4, 10.9	58 ± 2
DMNA	DTAB	2.3, 4.7, 7.0	2.3, 4.7, 7.0	88 ± 2
	TTAB	2.4, 4.7, 7.2	2.2, 4.5, 6.9	90 ± 2
	CTAB	1.4, 2.9, 4.3	1.4, 2.8, 4.1	94 ± 2

[a] The error bars on the *N* values can be found by using the error bars on the % bound values.

sub-cmc surfactant, in the experimental concentration of surfactant, and in 10 times the experimental concentration of surfactant for each of the three surfactants. The DMA concentration was 2 mM, and the DMNA concentration was 0.31 mM. Spectra were corrected for small variations in the concentrations of DMA and DMNA used to made each sample. The peak for substrate absorption in sub-cmc surfactant (representing unbound substrate, because no micelles are present below the critical micelle concentration) is always to the blue of the experimental solutions, and the absorption peak in high concentration surfactant (representing substrate completely bound to micelles) is always to the red of the experimental solutions, as shown in Figure 3.

The percent of substrate that was bound to the micelles was determined from the spectra by adding together the experimental spectra for unbound substrate (sub-cmc surfactant) and bound substrate (10x experimental surfactant concentration) to obtain the substrate spectrum at experimental surfactant concentration. To determine the binding constant, the bound spectrum was multiplied by $0 < x < 1$ and the unbound spectrum was multiplied by $(1 - x)$. x is the fraction of the substrate that is bound to the micelle. Results are reported in Table 2 as % bound. DMNA is much less soluble in water than DMA, and a higher percentage of DMNA is bound to the micelles than DMA.

In Table 2, the average number, *N*, of substrate molecules bound to each micelle is listed. The donor molecules are assumed to follow a Poisson distribution among the micelles. DMNA is less soluble in the micelles themselves than DMA. Therefore, the values of *N* for the DMNA samples are smaller than the values for DMA. Because two separate sets of samples were used in the experiments, one set for the time dependent up-conversion experiments and one for the fluorescence yield experiments, two sets of numbers are listed, *N* up-conversion and *N* yield.

Donor and acceptor radii were determined from molecular models. The hard sphere radius for each molecule was taken to be the radius of a sphere with the volume obtained from the molecular model. Radii used were 4.12 Å for ODRB, 3.09 Å for DMNA, and 2.75 Å for DMA. These values should be more accurate than previously used values that were based on crystal structures of similar molecules rather than the actual molecules.[8,9] The distance of closest approach between the donor and acceptor is 6.87 Å for ODRB/DMA and 7.21 Å for ODRB/DMNA. γ_o is the angle associated with this distance and varies with *R*, the micelle radius. The micelle radii are given in Table 1.[9,8]

R, the micelle radius, is defined as the distance from the center of the micelle to the center of the donor and acceptor molecule (see Figure 1B). Because DMA resides preferentially at the edge of the micelle hydrocarbon core, *R* was taken to be the core radius determined by the Tanford equation: $R = (1.5 + 1.265)T$ Å, where *T* is the number of carbons in the hydrocarbon tail.[94] The analytical theory requires that the headgroup shell must enclose all donors and acceptors completely. Both simulations and experiments predict a 5−9 Å thick surface region in micelles that has properties distinct from the core or surrounding water.[58,90,95−98] We choose to let $a_C = R - 4.12$ Å and the outer radius of the shell be $a_S = R + 4.12$ Å, so the shell thickness is the donor diameter.

TABLE 3: Acceptor Diffusion Characteristics and Donor Fluorescence Lifetime

substrate	micelle	τ_r, ps	η_{calcd}, cP	$D_{2D\ calcd}$, Å²/ns	τ, ns
DMA	CTAB	120 ± 20	10.3 ± 1.7	15.3 ± 2.5	1.78 ± 0.05
DMNA	DTAB	140 ± 20	8.2 ± 1.2	15.9 ± 2.3	1.78 ± 0.05
	TTAB	170 ± 20	10.0 ± 1.2	13.1 ± 1.5	1.84 ± 0.05
	CTAB	220 ± 20	12.9 ± 1.1	10.1 ± 0.9	1.89 ± 0.05

The optical and static dielectric constants for hexane, $\epsilon_{op} = \epsilon_{st} = 1.88$,[99] were used for the micelle's hydrocarbon core. For the water surrounding the micelles, $\epsilon_{op} = 1.77$ and $\epsilon_{st} = 78.3$.[99] The optical dielectric constant for the headgroup shell region did not significantly affect the fits, so $\epsilon_{op} = 1.9$ was assumed in all cases. The static dielectric constant of the headgroup shell will be discussed in detail in following sections. The dielectric constants are used to calculate both solvent reorganization energy and free energy of transfer in micelles.

The oxidation potentials of DMNA and DMA in acetonitrile vs SCE are 0.75 and 1.01 V, respectively.[100,101] The difference between the reduction potential of rhodamine B and the oxidation potential of DMA in acetonitrile has been measured by cyclic voltammetry and is 1.55 V.[9] These data were combined to calculate $(E^{ox} - E^{red})_{MeCN} = 1.29$ V, the difference in redox potentials in bulk solution for DMNA/ODRB. $\epsilon_{st} = 35.9$ is used as the static dielectric constant for bulk acetonitrile.[102] ν in eq 5 is the frequency at which the normalized donor absorption and fluorescence spectra cross. $\nu = 580$ nm for ODRB. These values were used in eq 5 to calculate ΔG for electron transfer on a micelle.

Translational diffusion constants of DMA and DMNA in acetonitrile were measured by cyclic voltammetry to be 305 and 252 Å²/ns, respectively. Details of the experiment have been presented previously.[2] Briefly, steady-state sigmoidal voltammograms were taken by using an Ensman Instrumentation 400 potentiostat and Bioanalytical Systems 10 μm platinum ultramicroelectrode. Limiting current was translated into diffusion constant following the example of Baur and Wightman.[103,104] In addition, rotational diffusion was determined from anisotropy measurements for both DMA and DMNA in each of the three micelle solutions and for DMNA in ethylene glycol. Anisotropy decays were obtained by time-correlated single photon counting. Details of the apparatus can be found elsewhere.[105] Excitation pulses were provided by a cavity-dumped dye laser running at 640 nm frequency-doubled to 320 nm for DMNA and 600 nm frequency-doubled to 300 nm for DMA. Photons were detected with a Hamamatsu microchannel plate detector in combination with a subtractive double monochromator tuned to 422 nm for DMNA and 370 nm for DMA. The instrument response was ~65 ps fwhm.

Orientational relaxation times, τ_r, are listed in Table 3. They were obtained from fluorescence anisotropy decays. Errors in τ_r are about 10 ps. The Debye expression for rotational diffusion can be used to solve for the effective viscosity in the headgroup region:[106]

$$\tau_r = \frac{4\pi a^3 \eta f_r}{3k_B T} \tag{17}$$

where k_B is Boltzmann's constant, *T* is temperature, *a* is the solute radius (the hard sphere radius was used), and f_r is the

correction factor for rotational diffusion of nonspherical molecules. $f_r = 0.566$ was determined by substituting known values of all parameters except f_r into eq 17 for rotation of DMNA in ethylene glycol. Because DMA and DMNA have essentially the same ratio of major/minor axes, this result is used for both DMA and DMNA calculations. This correction factor would be expected to apply for cases of slip boundary conditions, because slip boundary conditions apply to rotational diffusion in ethylene glycol.[107] Slip boundary conditions would also be expected for headgroup region because surfactant headgroups would not move readily with the solute. Calculated η's are listed for DMA and DMNA in the micelles in Table 3. The similarity between viscosities calculated for the same micelle using different substrates is encouraging given the error in rotational measurements, the simplicity of the Debye expression, and roughness of the f_r calculation.

These effective viscosities are used to calculate lateral diffusion constants in the headgroup regions using the Stokes−Einstein relation in two dimensions:[106]

$$D = \frac{k_B T}{4\pi a \eta f_t} \tag{18}$$

where f_t is the correction factor for translational diffusion of nonspherical molecules. For stick boundary conditions, f_t can be calculated from eq 18 by using measured translational diffusion coefficients and other known parameters in acetonitrile. Because diffusion in acetonitrile is in three dimensions rather than two, the 4 is replaced by a 6 in eq 18. With this modification, $f_t = 1.200$ and 1.288 were calculated for DMA and DMNA, respectively. Because slip boundary conditions would be more appropriate for a micelle headgroup region, these numbers must be modified. From molecular models, the oblate spheroid major and minor axes were measured to be 9.0 and 2.5 Å for DMA and 9.2 and 2.5 Å for DMNA (the length across the benzene ring and $N(CH_3)_2$ in DMA is about the same as the length across the naphthyl structure in DMNA). From these numbers, the slip/stick correction factor can be determined.[108] Correction factors for slip boundary conditions were calculated to be $f_t = 0.753$ and 0.808 for DMA and DMNA, respectively. Finally, lateral diffusion constants, D, in the micelle headgroup regions can be calculated from eq 17 by using the estimated viscosities calculated from eq 16, using slip correction factors. The results are listed in Table 3.

The calculated lateral diffusion coefficients are approximate. The estimates and approximations made in the calculations lead to uncertainty in the values given in Table 3. The error bars given in Table 3 are based on uncertainties in the actual measurements. However, systematic errors related to the use of eqs 16 and 17 cannot be ruled out. Nonetheless, the predicted trends should be correct, and the true diffusion constants are expected to agree with those listed in Table 3 within a factor of 2. Because ODRB molecules are tethered into the micelles, their diffusion is insignificant compared to that of DMA and DMNA and is not considered in the data analysis.

In this study, both time-dependent fluorescence decays and fluorescence yield data were collected. Experimental details can be found elsewhere.[9] The fluorescence up-conversion technique was used to take the time-dependent data. The sample was excited with a 30-ps, 568-nm laser pulse. The fluorescence is summed with a time-delayed 882-nm pulse to time-resolve the decay. Steady-state fluorescence yield measurements were corrected for ODRB concentration and compared to fluorescence from a sample without acceptors. Fluorescence lifetimes, τ, listed in Table 3, were measured in samples containing no donor molecules.

IV. Results and Discussion

For each of the four micelle systems presented in this paper, fluorescence up-conversion and fluorescence yield data for three or four different acceptor concentrations were fit simultaneously. Experimentally determined values for β in a number of different electron-transfer systems fall in a range centered around 1 $Å^{-1}$.[17,46,64,109,110] In experiments in liquids using R3B and DMA, the data were fit well with $\beta = 1.0$ $Å^{-1}$.[2,3] Therefore, in fitting the data, β is not an adjustable parameter; it is taken to be 1.0 $Å^{-1}$. Diffusion constants listed in Table 3 were used. As discussed in section II.D, the radial distribution function, $g(r)$, and the hydrodynamic effect, $D(r)$, were included in the calculations.

The electronic coupling between rhodamine 3B (ODRB with a 2-carbon rather than a 18-carbon hydrocarbon tail) and DMA has already been measured in a number of liquids with excellent agreement between experiment and calculations.[3,2] The liquid data could be fit with $J_o = 300$ cm^{-1} and $\beta = 1.0$ $Å^{-1}$ when inner-sphere reorganization energy is $\lambda_i = 0.10$ eV. The value of λ_i was taken from values calculated in the literature for similar molecules. Therefore, these values are used as constants in fitting the DMA/ODRB data in this work. For the DMA/ODRB in CTAB system, the only remaining unknown parameters are the static dielectric constant of the headgroup shell region, $\epsilon_{st,S}$, and the effective solvent diameter that enters into $g(r)$ and $D(r)$.

When DMA/ODRB/CTAB data are analyzed without inclusion of $g(r)$, all values of $\epsilon_{st,S}$ result in poor fits to the data. The calculated decays are always slower than the experimental measurements. However, when $g(r)$ is included, it is possible to fit the time and yield data simultaneously when the hard sphere solvent diameter is 4 Å $< \sigma <$ 10 Å. Fits are not sensitive to the inclusion of $D(r)$ or to the solvent diameter used for $D(r)$ calculations. For liquids, $D(r)$ has the strongest effect in cases of fast diffusion.[2] The diffusion in the micelle systems studied here is slow enough that the hydrodynamic effect has no discernible influence on the data. It is included in calculations, using the same solvent diameter as for $g(r)$. However, calculations are indistinguishable from curves calculated with no hydrodynamic effect. When $g(r)$ is included, excellent fits are obtained to the time and yield data for $\epsilon_{st,S} = 4-7$, for $\sigma = 4-10$ Å (ϵ_{st} decreases as σ increases). Figure 4 shows data and fits for the DMA/ODRB/CTAB system. These fits are unique, and parameters outside these ranges do not give acceptable fits to the data. In the fits shown, $\sigma = 5$ Å was used. This corresponds approximately to the size of the surfactant headgroup, a reasonable value. The dielectric constant of 6, which is obtained with $\sigma = 5$ Å, is a reasonable value. Neutron scattering experiments show that CTAB has some water in the headgroup region but significantly less than in DTAB.[90] The value of $\epsilon_{st,S}$ obtained is substantially greater than that of the hydrocarbon core but substantially less than that of water.

The properties of the CTAB headgroup region that were determined from fits to the DMA/ODRB/CTAB data should apply equally well for the DMNA/ODRB/CTAB system. For the DMNA/ODRB system, the electronic coupling between the donor/acceptor pair is not known from previous experiments. However, if β is again taken to be 1 $Å^{-1}$, there is only one fitting parameter, J_o, because σ and $\epsilon_{st,S}$ were determined. When these parameters are fixed at $\sigma = 5$ Å and $\epsilon_{st,S} = 6$, very good fits to the DMNA/CTAB data are obtained for $J_o = 70$ cm^{-1}.

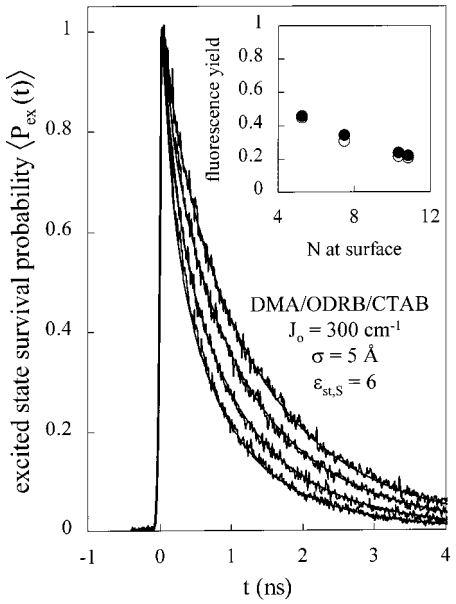

Figure 4. Data and fits for ODRB and four concentrations of DMA in CTAB. $J_o = 300$ cm^{-1}, $\beta = 1$ Å^{-1}, $\sigma = 5$ Å, and $\epsilon_{st,S} = 6$. Inset shows fluorescence yield data (○) and fits (●).

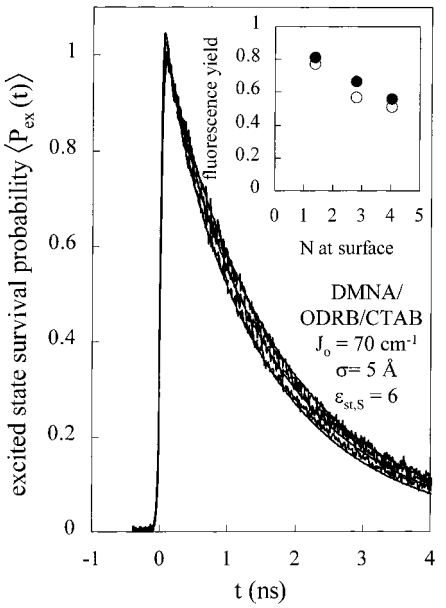

Figure 5. Data and fits for ODRB and three concentrations of DMNA in CTAB. $J_o = 70$ cm^{-1}, $\beta = 1$ Å^{-1}, $\sigma = 5$ Å, and $\epsilon_{st,S} = 6$. Inset shows fluorescence yield data (○) and fits (●).

Figure 5 shows data and fits for DMNA/ODRB/CTAB. J_o is smaller for DMNA/ODRB than for DMA/ODRB. A possible explanation for this is discussed below.

Using $J_o = 70$ cm^{-1}, fits to the DMNA/ODRB/TTAB and DMNA/ODRB/DTAB data sets can be obtained using the headgroup properties σ and $\epsilon_{st,S}$ for TTAB and DTAB as the adjustable parameters. Figures6 and 7 show data and fits for DMNA and ODRB in TTAB and DTAB, respectively. It is only possible to fit the DTAB and TTAB data with $J_o = 70$ cm^{-1} if $g(r)$ is included in the calculations. Both sets of data can only be fit when 4 Å $< \sigma <$ 8 Å, with $20 < \epsilon_{st,S} < 78$. The large possible range of dielectric constants signifies that the headgroup region is very polar in these micelles. The fits are very good although there is some error in the yields. Given the uncertainties, $\epsilon_{st,S}$ may be the same in the two micelles. The calculated curves in the figures are for $\epsilon_{st,S} = 30$. Neutron scattering shows

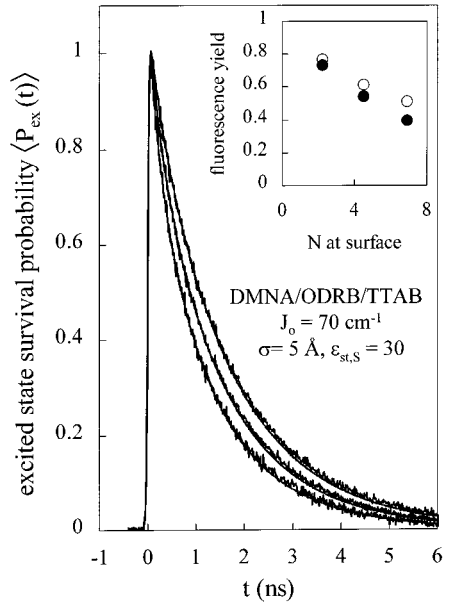

Figure 6. Data and fits for ODRB and three concentrations of DMNA in TTAB. $J_o = 70$ cm^{-1}, $\beta = 1$ Å^{-1}, $\sigma = 5$ Å, and $\epsilon_{st,S} = 30$. Inset shows fluorescence yield data (○) and fits (●).

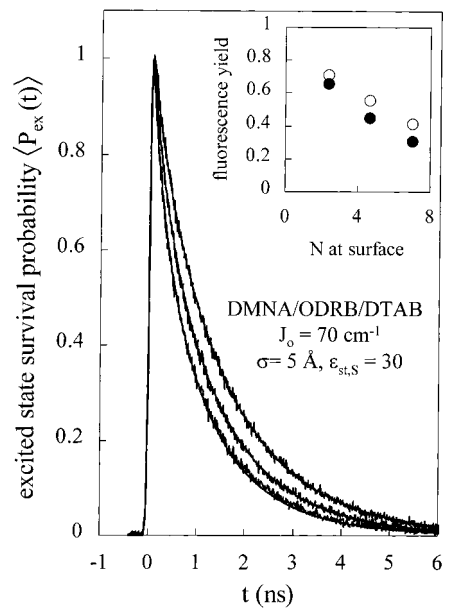

Figure 7. Data and fits for ODRB and three concentrations of DMNA in DTAB. $J_o = 70$ cm^{-1}, $\beta = 1$ Å^{-1}, $\sigma = 5$ Å, and $\epsilon_{st,S} = 30$. Inset shows fluorescence yield data (○) and fits (●).

that there is more water penetration into the headgroup regions of DTAB than of CTAB.[90] Increased water in the headgroup region is consistent with increased $\epsilon_{st,S}$. Furthermore, the fits require the same values of σ to enter $g(r)$ in all three micelles. If σ is determined by the size of the surfactant headgroups, as is suggested by the value of σ, it is reasonable that the same σ should emerge for fits of data for the three different micelles.

Data exhibiting the greatest amount of transfer can be fit most uniquely and lead to the most reliable conclusions. The lack of totally unique fits is partially due to the difficulty involved in fitting the exact shape of the distinct curves. Increased transfer occurs for samples with higher donor concentrations, which are more sensitive to the effects of $g(r)$ and $D(r)$. As a result, the first fits that were performed were for DMA/ODRB/CTAB, which have the highest bound acceptor concentrations. These results demonstrate that $g(r)$ has a significant impact on electron

transfer in the headgroup regions of micelles. In addition, they suggest that groups in the headgroup region of diameter 4 Å or larger determine the solute $g(r)$ and that the effective dielectric constant of the headgroup region is approximately 6. The other two sample sets with large amounts of electron transfer and the most reliable data are DMNA/ODRB/TTAB and DMNA/ODRB/DTAB. Fits to these data indicate that the effective dielectric constant in the headgroup region of the micelles increases as micelle size decreases. This is in agreement with neutron scattering studies that have shown that there are more methylene units in contact with water in the smaller trimethylammonium bromide micelles and that water penetrates deeper into the smaller micelles.[90]

For all of the micelle electron-transfer systems studied, the three-region model (core, headgroup, water) is necessary. Calculations performed with a simpler two-region model in which the headgroup region was given the same dielectric properties, as either the surrounding water or the hydrocarbon core, cannot fit the data, so the entire three-region model is necessary.

Although many of the parameters that are included in fitting the micelle data are not precisely known, the qualitative results are robust. If the substrate percent bound (Table 2) is changed by ±20% or if the diffusion constant is changed by ±20%, it is still only possible to fit the DMA/CTAB data using $g(r)$ with $\sigma \approx 5$ Å. It has been shown that $g(r)$ can have a strong influence on electron-transfer dynamics in liquids.[3,2] Therefore, solvent structure would be expected to play a role in electron transfer in micelles as well. Part of the reason is that $g(r)$ exerts most of its influence within a few angstroms of contact, exactly the same distance scale on which electron-transfer occurs.

Although the structure in the headgroup region of micelles is not expected to be modeled precisely with a three-dimensional hard sphere liquid description, the model is a useful approximation because it does have the required oscillatory distance dependence with a period of one solvent diameter. Use of the three-dimensional hydrodynamic effect for the headgroup region of a micelle is also approximate, but it does provide the expected decrease in diffusion at short distance. Slip boundary conditions are used for diffusion in the headgroup region of a micelle because a large number of the surrounding solvent "molecules" are surfactant headgroups that are bound to the micelle and will not readily move with the diffusing substrate molecules. One of the primary effects of including solvent structure is to increase the amount of short-time electron transfer by increasing the donor concentration near contact. When the DMA/ODRB/CTAB data are fit without $g(r)$, it is possible to fit the time decays, but the fluorescence yield calculations predict far too little electron transfer. When $g(r)$ is included, both time and yield data fit quite well. The fact that a hard sphere solvent diameter of ~5 Å is required to model the donor−acceptor distance distribution suggests that the surfactant headgroups, rather than water molecules, play the major role in determining the solute $g(r)$. Water molecules have a radius much smaller than 5 Å, whereas the surfactant trimethylammonium headgroups have a radius close to 5 Å.

In a previous study of DMA/ODRB in DTAB, TTAB, and CTAB, it was assumed that all of the DMA placed in the experimental samples was bound to the micelles.[8] g(r) and D(r) were not included in those calculations. The results presented here show that a significant portion of DMA is not bound and that g(r) is important. Therefore, the analysis present here provides an improved description of electron transfer in these micelle systems.

The value for J_o found for DMA/R3B in a number of liquids is 300 cm^{-1}.[2,3] This value is somewhat dependent on the choice of λ_i. λ_i used in the calculations was taken from literature values of similar molecules.[2,111−114] Changing λ_i does not affect the shape or quality of the fits, but changes the J_o value resulting from fits. J_o values determined from fits can change by ±50% for a range of reasonable values of λ_i.[2] However, λ_i is an intrinsic property of a pair of molecules, and J_o values determined in different surroundings for the same donor/acceptor pair using the same λ_i should be comparable. When λ_i was fixed at 0.10 eV in the liquid studies, J_o was found to be consistent for all of the liquids.[2,3] R3B and ODRB are both esters and only differ by the length of the alkyl chain on the ester. Therefore, J_o was taken to be the same for DMA/R3B and DMA/ODRB. J_o for DMNA/ODRB was found to be 70 cm^{-1}. The difference in J_o for the two hole acceptors can arise for a number of reasons. DMA and DMNA could have different λ_i values, which would result in different J_os. DMNA is larger than DMA. J_o is the electronic coupling matrix element at contact. In the theory, the distance is the center-to-center distance of spheres. The larger DMNA is thus farther away from the ODRB at contact than is DMA. In some sense then, the direct comparison of the J_o values is not quite correct. If the DMNA J_o is extrapolated to the shorter contact distance of DMA using $\beta = 1$ Å, its J_o increases to 100 cm^{-1}. Furthermore, if the spherical size estimates of the two molecules, which are based on molecular models, are off, the values of J_o will change.

A more important effect may be the difference not only in the sizes of DMA and DMNA but also in their shapes. Both are electron donors. In contrast to the spherical model used in the calculations, the electronic interaction responsible for the electron transfer is not evenly distributed throughout the molecules. It is likely that the portion of the molecules in the vicinity of the amine moiety dominates the electron-transfer interaction.[115,116] In the calculations, because of the spherical model, there is no angle average. In these nonspherical molecules with off-center electron-donation portions, the angle-averaged donor−acceptor electronic coupling could be very different. If the electron transfer in both molecules were dominated by the part of the molecules close to the amine, then an orientational average will place the amine portion of DMNA on average significantly farther away from the ODRB than the amine portion of DMA. This occurs because the DMNA is more elongated than DMA. Both have the same closest approach distance, but DMNA has many orientational configurations that place the amine substantially further away. The increased orientationally averaged contact distance of the amine portion of DMNA could result in a significant reduction in J_o.

The model used to describe the electron transfer in micelles contains a variety of features that were found to be necessary to describe the data. It is worth mentioning some aspects of the problem that were not included. The polyelectrolyte nature of micelle surface (charged headgroups and counterions) has not been included in the model. However, in other systems, it has been shown that electrolyte contributions to electrostatic potentials are minor compared to overall polar solvent effects.[70] Another factor is the orientational dependence of the electron transfer rate. The relatively fast orientational relaxation of acceptor molecules (see Table 3) will remove the orientational dependence of the transfer rate on longer time scales. However, even at shorter times, a theoretical study has shown that when an orientational average is combined with a distance average, the time dependence of the transfer is almost indistinguishable from that involving the distance dependence alone.[117] It was

noted above that the anisotropic shape of the molecules, particularly DMNA, could result in the effective contact distance being greater than the center-to-center distance, thereby, reducing the magnitude of the contact electronic interaction, J_o. The three region (water, headgroup, core) description of the micelle in terms of three dielectric constants is necessary to account for inhomogeneous nature of the micelle structure experienced by the donors and acceptors. Assigning dielectric constants to the water and the core is reasonable. However, the headgroup region is itself inhomogeneous in structure. The dielectric constant associated with the headgroup region is probably best viewed as an effective dielectric constant.

V. Concluding Remarks

Electron transfer has been studied for two different donor/acceptor pairs located in the headgroup regions of three different micelles. Time-dependent fluorescence and fluorescence yield data were taken for several concentrations of acceptors for each of the four systems studied. The data were analyzed by using a theory that included the important features of the micelle systems and the electron transfer process. The Marcus distance dependent transfer rate was used, but it was modified to account for the heterogeneous nature of the micelle dielectric environment. Important additions to the theory previously used to describe electron transfer in micelles are the inclusion of the radial distribution function of the acceptors about the donor and the hydrodynamic effect. It was found to be impossible to fit the data in the DMA/ODRB/CTAB systems without including $g(r)$. When $g(r)$ is included, excellent fits to both time and yield data were obtained. Fits yield information about the dielectric properties of a CTAB micelle and structural characteristics of solutes in the headgroup region. Using this information, good fits are obtained for the DMNA/ODRB/CTAB data with the donor−acceptor electronic coupling as a single adjustable parameter. Using the fit value of the electronic coupling, data in DMNA/ODRB/TTAB and DMNA/ODRB/DTAB systems can also be fit, and the results provide additional information about the headgroup regions of the micelles. The consistency of the results and the quality of the fits support the model. It is remarkable that in such complex systems, with heterogeneous dielectric environments, solute diffusion, structured local environments, and distance-dependent transfer, it is possible to fit the shape and magnitude of data for several donor concentrations in systems with different acceptor molecules in three different types of micelles. Fits to the data can only be obtained when a realistic model includes the effects of local solvent structure and a three-region micelle system with dielectric properties of the micelle headgroup region being between those of hydrocarbon and water.

Beyond the detailed analysis of the particular systems studied here, the results and the theory used to analyze them demonstrate the importance of treating complex systems for what they are, complex. Marcus[38,40,41,63−65] and others showed that the distance dependence of electron transfer could not be described as a simple exponential representing the falloff of the electronic interaction. It is also necessary to include the distance dependence of the reorganization energy and the free energy change. For donors and acceptors diffusing in a liquid, it is not sufficient to consider electron transfer and geminate recombination as only occurring at contact, nor is it sufficient to describe the liquid as a homogeneous continuum. Proper ensemble averages over the spatial distribution of donors and acceptors are required,[50,51,55,118−120] and the inclusions of the radial distribution function and the hydrodynamic effect are necessary.[2,3,5,51] The electron-transfer problem becomes even more intricate for systems with complex geometries as evidenced by the recent activity describing electron transfer in DNA.[21−26] As systems (e.g., DNA) become more complex, there is a natural tendency to simplify the description, leaving out aspects that are known to be important in other contexts.[20]

The work presented here on micelles is an attempt to describe electron-transfer dynamics in a finite volume, restricted topology system, in a manner that accounts for the major aspects of the problem. The theory is not a perfect description of electron transfer in micelles, but it does include all of the factors that are known to be necessary to describe electron transfer in liquids plus additional components that are necessary to capture the essential nature of the micelle problem. The experiments and theory point the way to a deeper understanding of electron transfer in complex systems.

Acknowledgment. This work was supported by the Department of Energy, Office of Basic Energy Sciences (Grant DE-FG03-84ER13251). We thank Professor Laurence S. Romsted, Rutgers University, for providing a great deal of input on methods for determining the binding constants of the acceptors to the micelles. We also thank Dr. Xueying Huang for help with the anisotropy experiments.

Appendix A. Analytical Solution of Integrals

The integrations necessary to calculate the solvent reorganization energy and free energy of transfer can be performed analytically when all space is comprised of a solvent and spherical regions with different dielectric properties whose surfaces do not intersect with each other or with the donor and acceptor sphere surfaces.[8,20,68] In addition, the donor and acceptor must be contained within the same dielectric region. In other cases, the integrals must be evaluated numerically. If one of the spherical regions is completely contained within another (as in the core and shell regions of the micelle, Figure 1B), the contribution of the larger sphere over the volume of the smaller sphere must be subtracted from the total, as in the core and shell regions of the micelle. Calculations can also be performed analytically for the case in which the donor and acceptor spheres are both contained within third sphere, as in the micelle case.

In all of these cases, the following analytical solutions to the integrals can be used:[8,68]

$$\frac{1}{4\pi}\int_{\infty-\upsilon_D-\upsilon_A}(d\mathbf{E}_D \pm a\mathbf{E}_A)^2\,dV = \frac{d^2}{4\pi}\int_{\infty-\upsilon_D}\mathbf{E}_D{}^2\,dV + \frac{a^2}{4\pi}\int_{\infty-\upsilon_A}\mathbf{E}_A{}^2\,dV \pm \frac{da}{2\pi}\int_{\infty-\upsilon_D-\upsilon_A}\mathbf{E}_D\mathbf{E}_A\,dV - \frac{d^2}{4\pi}\int_{\upsilon_A}\mathbf{E}_D{}^2\,dV - \frac{a^2}{4\pi}\int_{\upsilon_D}\mathbf{E}_A{}^2\,dV = \frac{d^2}{a_D} + \frac{a^2}{a_A} \pm \frac{2da}{r} - d^2f(r,a_A) - a^2f(r,a_D) \quad \text{(A1)}$$

and

$$\frac{1}{4\pi}\int_{\upsilon_q}(d\mathbf{E}_D \pm a\mathbf{E}_A)^2\,dV = + \frac{d^2}{4\pi}\int_{\upsilon_q}\mathbf{E}_D{}^2\,dV + \frac{a^2}{4\pi}\int_{\upsilon_q}\mathbf{E}_A{}^2\,dV \pm \frac{da}{2\pi}\int_{\upsilon_q}\mathbf{E}_D\mathbf{E}_A\,dV = d^2f(R_{Dq},a_q) + a^2f(R_{Aq},a_q) \pm daL(\rho(a_q),\gamma_q) \quad \text{(A2)}$$

where d and a are constants. υ_q and a_q denote the volume and radius, respectively, of a spherical dielectric region q or a donor/

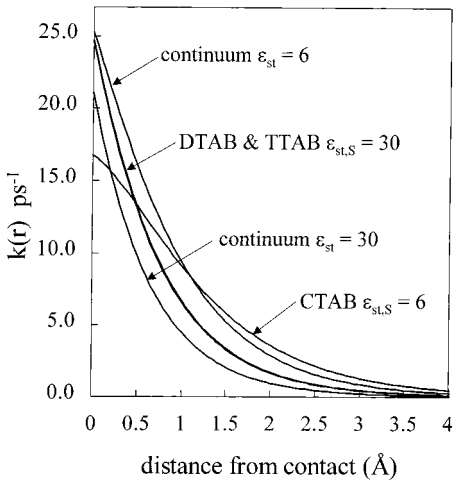

Figure 8. Distance dependent electron-transfer rate constants vs distance for best fits to DMNA/ODRB data in CTAB, TTAB, and DTAB, using a three-region model with $\epsilon_{st,S} = 6$, 30, and 30, respectively. $J_o = 70$ cm^{-1} and $\beta = 1$ Å^{-1}. The Marcus rate is calculated using eqs 2, 3−8, and A1−A4 to calculate λ and ΔG for the micelle systems. Calculations are also shown for electron transfer in a continuum with the same dielectric constants as the headgroup shell region. Continuum calculations are very different from micelle calculations with the same shell dielectric constants. The analogous figure in a previous paper[8] was incorrect and did not correct $\Delta E°$ for dielectric constant in the continuum calculations.

acceptor sphere *D*/*A*. *r* is the donor−acceptor center-to-center separation distance. $\rho(a_q) = a_q/\sqrt{R_{Dq}R_{Aq}}$, where $R_{Dq/Aq}$ are the center-to-center distances between the donor/acceptor and a spherical region q. γ_q is the angle between lines drawn between the centers of the donor and acceptor molecules and the center of the sphere q, with $\cos(\gamma_q) = (R_{Dq}^2 + R_{Aq}^2 - r^2)/(2R_{Dq}R_{Aq})$. *f* are the Kharkats correction factors for donor and acceptor volumes:[69]

$$f(r,a_q) = \frac{a_q}{2|r^2 - a_q^2|} - \frac{r - a_q}{4r|r - a_q|}\ln\frac{r + a_q}{|r - a_q|} \quad \text{(A.3)}$$

Finally,

$$L(\rho(a_q),\gamma_q) = \frac{1}{\sqrt{R_{Dq}R_{Aq}}}\sum_{n=0}^{\infty}\left(1 \mp \frac{1}{2n+1}\right)\rho^{\pm(2n+1)}P_n(\cos\gamma) \quad \text{(A.4)}$$

where $P_n(x)$ denote Legendre polynomials. The upper sign corresponds to $\rho(a_q) < 1$, when the donor and acceptor are outside the spherical region q. The lower sign applies when the donor and acceptor spheres are both contained within region q.

Appendix B. Effects of Heterogeneity

Figure 8 shows the impact of including the core, shell, and water dielectric regions in λ and ΔG calculations for electron transfer in a micelle headgroup region. It shows the distance dependence of the electron transfer rates used for best fits to DMNA/ODRB data in three micelles, along with calculations for electron transfer in a continuum with the same dielectric constant as the headgroup shell region. The continuum and micelle rates have similar shapes but are very different in amplitude, even when the donor and acceptor are embedded in a region of the same dielectric constant. Including the core and water regions makes a significant difference in the rate calculations. Properly modeling the heterogeneous dielectric nature of the micelle system can lead to very different calculated distance-dependent rate constants compared to a continuum approach and can have a significant impact on the results of data analysis.

References and Notes

(1) *Electron transfer−from isolated molecules to biomolecules*; Jortner, J., Bixon, M., Eds.; J. Wiley: New York, 1999; Vol. 106−107.
(2) Tavernier, H. L.; Kalashnikov, M. M.; Fayer, M. D. *J. Chem. Phys.* **2000**, *113*, 10 191.
(3) Tavernier, H. L.; Fayer, M. D. *J. Chem. Phys.* **2001**, *114*, 4552.
(4) Weidemaier, K.; Tavernier, H. L.; Swallen, S. F.; Fayer, M. D. *J. Phys. Chem. A* **1997**, *101*, 1887.
(5) Swallen, S. F.; Weidemaier, K.; Tavernier, H. L.; Fayer, M. D. *J. Phys. Chem.* **1996**, *100*, 8106.
(6) Iwai, S.; Murata, S.; Tachiya, M. *J. Chem. Phys.* **1998**, *109*, 5963.
(7) Burel, L.; Mostafavi, M.; Murata, S.; Tachiya, M. *J. Phys. Chem. A* **1999**, *103*, 5882.
(8) Tavernier, H. L.; Barzykin, A. V.; Tachiya, M.; Fayer, M. D. *J. Phys. Chem. B* **1998**, *102*, 6078.
(9) Weidemaier, K.; Tavernier, H. L.; Fayer, M. D. *J. Phys. Chem. B* **1997**, *101*, 9352.
(10) Aota, H.; Araki, S.; Morishima, Y.; Kamachi, M. *Macromolecules* **1997**, *30*, 4090.
(11) Borsarelli, C. D.; Cosa, J. J.; Previtali, C. M. *Photochem. Photobiol.* **1998**, *68*, 438.
(12) Hackett, J. W. I.; Turro, C. *J. Phys. Chem. A* **1998**, *102*, 5728.
(13) Barzykin, A. V.; Seki, K.; Tachiya, M. *J. Phys. Chem. B* **1999**, *103*, 9156.
(14) Pal, S. K.; Mandal, D.; Sukul, D.; Bhattacharyya, K. *Chem. Phys.* **1999**, *249*, 63.
(15) Hammarström, L.; Norrby, T.; Stenhagen, G.; Martensson, J.; Akermark, B.; Almgren, M. *J. Phys. Chem. B* **1997**, *101*, 7494.
(16) Regan, J. J.; Onuchic, J. N. Electron-transfer tubes. In *Electron transfer − from isolated molecules to biomolecules*; Joshua Jortner, M. B., Ed.; J. Wiley: New York, 1999; Vol. 107; p 497.
(17) Gray, H. B.; Winkler, J. R. *Annu. Rev. Biochem.* **1996**, *65*, 537.
(18) Hu, Y. Z.; Tsukiji, S.; Shinkai, S.; Oishi, S.; Hamachi, I. *J. Am. Chem. Soc.* **2000**, *122*, 241.
(19) DiBilio, A. J.; Dennison, C.; Gray, H. B.; Ramirez, B. E.; Sykes, A. G.; Winkler, J. R. *J. Am. Chem. Soc.* **1998**, *120*, 7551.
(20) Tavernier, H. L.; Fayer, M. D. *J. Phys. Chem. B* **2000**, *104*, 11541.
(21) Lewis, F. D.; Wu, T.; Zhang, Y.; Letsinger, R. L.; Greenfield, S. R.; Wasielewski, M. R. *Science* **1997**, *277*, 673.
(22) Brun, A. M.; Harriman, A. *J. Am. Chem. Soc.* **1992**, *114*, 3656.
(23) Dandliker, P. J.; Nunez, M. E.; Barton, J. K. *Biochemistry* **1998**, *37*, 6491.
(24) Kelley, S. O.; Barton, J. K. *Science* **1999**, *283*, 375.
(25) Lewis, F. D.; Kalgutkar, R. S.; Wu, Y. S.; Liu, X. Y.; Liu, J. Q.; Hayes, R. T.; Miller, S. E.; Wasielewski, M. R. *J. Am. Chem. Soc.* **2000**, *122*, 12346.
(26) Giese, B.; Wessely, S.; Spormann, M.; Lindemann, U.; Meggers, E.; Michel-Beyerle, M. E. *Angew. Chem., Int. Ed. Engl.* **1999**, *38*, 996.
(27) Morishima, Y.; Aota, H.; Saegusa, K.; Kamachi, M. *Macromolecules* **1996**, *29*, 6505.
(28) Fox, M. A. "Photoinduced Electron Transfer in Arranged Media". In *Topics in Current Chemistry*; Mattay, J., Ed.; Springer-Verlag: Berlin, 1991; Vol. 159; p 67.
(29) Nakagaki, M.; Komatsu, H.; Tanaka, H.; Handa, T. *Bull. Chem. Soc. Jpn.* **1986**, *59*, 3007.
(30) Hammarström, L.; Berglund, H.; Almgren, M. *J. Phys. Chem.* **1994**, *98*, 9588.
(31) Hubig, S. M. *J. Lumin.* **1991**, *47*, 137.
(32) Lerebours, B.; Chevalier, Y.; Pileni, M. P. *Chem. Phys. Lett.* **1985**, *117*, 89.
(33) Chandler, D. *Introduction to Modern Statistical Mechanics*; Oxford University Press: New York, 1987.
(34) Stryer, L. *Annu. Rev. Biochem.* **1978**, *47*, 819.
(35) Ediger, M. D.; Domingue, R. P.; Fayer, M. D. *J. Chem. Phys.* **1984**, *80*, 1246.
(36) Peterson, K. A.; Zimmt, M. B.; Linse, S.; Domingue, R. P.; Fayer, M. D. *Macromolecules* **1987**, *20*, 168.
(37) Ediger, M. D.; Fayer, M. D. *J. Chem. Phys.* **1983**, *78*, 2518.
(38) Sutin, N. Nuclear and Electronic Factors in Electron Transfer: Distance Dependence of Electron-Transfer Rates. In *Electron Transfer in Inorganic, Organic, and Biological Systems*; Bolton, J. R., Mataga, N., McLendon, G., Eds.; The American Chemical Society: Washington, 1991; p 25.
(39) Wasielewski, M. R. Distance Dependencies of Electron Transfer Reactions. In *Photoinduced Electron Transfer. Part A: Conceptual Basis*; Fox, M. A., Chanon, M., Eds.; Elsevier: New York, 1988; p 161.
(40) Marcus, R. A. *J. Chem. Phys.* **1956**, *24*, 966.

(41) Marcus, R. A. *J. Chem. Phys.* **1956,** *24*, 979.
(42) Rehm, D.; Weller, A. *Isr. J. Chem.* **1970**, *8*, 259.
(43) Arkin, M. R.; Stemp, E. D. A.; Turro, C.; Turro, N. J.; Barton, J. K. *J. Am. Chem. Soc.* **1996**, *118*, 2267.
(44) Shioyama, H.; Takami, A.; Mataga, N. *Bull. Chem. Soc. Jpn.* **1985**, *58*, 1029.
(45) Liu, Y. P.; Newton, M. D. *J. Phys. Chem.* **1994**, *98*, 7162.
(46) Miller, J. R.; Beitz, J. V.; Huddleston, R. K. *J. Am. Chem. Soc.* **1984**, *106*, 5057.
(47) Murata, S.; Matsuzaki, S. Y.; Tachiya, M. *J. Phys. Chem.* **1995**, *99*, 5354.
(48) Inokuti, M.; Hirayama, F. *J. Chem. Phys.* **1965**, *43*, 1978.
(49) Tachiya, M. *Radiat. Phys. Chem.* **1983**, *21*, 167.
(50) Dorfman, R. C.; Fayer, M. D. *J. Chem. Phys.* **1992**, *96*, 7410.
(51) Swallen, S. F.; Weidemaier, K.; Fayer, M. D. *J. Chem. Phys.* **1996**, *104*, 2976.
(52) Deutch, J. M.; Felderhof, B. U. *J. Chem. Phys.* **1973**, *59*, 1669.
(53) Zwanzig, R. *Adv. Chem. Phys.* **1969**, *15*, 325.
(54) Rice, S. A. *Diffusion-Limited Reactions*; Elsevier: Amsterdam, 1985.
(55) Lin, Y.; Dorfman, R. C.; Fayer, M. D. *J. Chem. Phys.* **1989**, *90*, 159.
(56) Dorfman, R. C.; Lin, Y.; Fayer, M. D. *J. Phys. Chem.* **1990**, *94*, 8007.
(57) Lindman, B. Structural Aspects of Surfactant Micellar Systems. In *Surfactants*; Tadros, T. F., Ed.; Academic Press: Orlando, 1984; p 83.
(58) Reiss-Husson, F.; Luzzati, V. *J. Phys. Chem.* **1964**, *68*, 3504.
(59) Karaborni, S.; O'Connell, J. P. *J. Phys. Chem.* **1990**, *94*, 2624.
(60) Gelbart, W. M.; Ben-Shaul, A. *J. Phys. Chem.* **1996**, *100*, 13169.
(61) Weidemaier, K.; Fayer, M. D. *J. Phys. Chem.* **1996**, *100*, 3767.
(62) Weidemaier, K.; Fayer, M. D. *J. Chem. Phys.* **1995**, *102*, 3820.
(63) Marcus, R. A. *Annu. Rev. Phys. Chem.* **1964**, *15*, 155.
(64) Marcus, R. A.; Sutin, N. *Biochim. Biophys. Acta* **1985**, *811*, 265.
(65) Bolton, J. R.; Archer, M. D. Basic Electron-Transfer Theory. In *Electron Transfer in Inorganic, Organic, and Biological Systems*; Bolton, J. R., Mataga, N., McLendon, G., Eds.; The American Chemical Society: Washington, 1991; p 7.
(66) Wang, Z.; Tang, J.; Norris, J. R. *J. Chem. Phys.* **1992**, *97*, 7251.
(67) Rips, I.; Jortner, J. *J. Chem. Phys.* **1987**, *87*, 6513.
(68) Barzykin, A. V.; Tachiya, M. *Chem. Phys. Lett.* **1998**, *285*, 150.
(69) Kharkats, Y. I. *Electrokhimiya* **1973**, *9*, 881.
(70) Marcus, R. A. Theory and Applications of Electron Transfers at Electrodes and in Solution. In *Special Topics in Electrochemistry*; Rock, P. A., Ed.; Elsevier: Amsterdam, 1977; p 161.
(71) Tachiya, M. *Chem. Phys. Lett.* **1994**, *230*, 491.
(72) Weller, A. *Z. Physik. Chem. NF* **1982**, *133*, 93.
(73) Wolynes, P. G.; Deutch, J. M. *J. Chem. Phys.* **1976**, *65*, 450.
(74) Northrup, S. H.; Hynes, J. T. *J. Chem. Phys.* **1979**, *71*, 871.
(75) Throop, G. J.; Bearman, R. J. *J. Chem. Phys.* **1965**, *42*, 2408.
(76) Percus, J. K. *Phys. Rev. Lett.* **1962**, *8*, 462.
(77) Thiele, E. *J. Chem. Phys.* **1963**, *39*, 474.
(78) Wertheim, M. S. *Phys. Rev. Lett.* **1963**, *10*, 321.
(79) Percus, J. K.; Yevick, G. Y. *Phys. Rev.* **1958**, *120*, 1.
(80) Smith, W. R.; Henderson, D. *Mol. Phys.* **1970**, *19*, 411.
(81) Verlet, L.; Weis, J. J. *Phys. Rev. A* **1972**, *5*, 939.
(82) Hansen, J. P.; McDonald, I. R. *Theory of Simple Liquids*; Academic Press: London, 1976.
(83) McQuarrie, D. A. *Statistical Mechanics*; Harper & Row: New York, 1976.
(84) Andersen, H. C., private communication.
(85) Eriksson, J. C.; Gillberg, G. *Acta Chem. Scand.* **1966**, *20*, 2019.
(86) Lianos, P.; Lang, J.; Strazielle, C.; Zana, R. *J. Phys. Chem.* **1982**, *86*, 1019.
(87) Lianos, P.; Lang, J.; Sturm, J.; Zana, R. *J. Phys. Chem.* **1984**, *88*, 819.
(88) Hein, N.; Sitnikov, R.; Furo, I.; Henriksson, U.; Regev, O. *J. Phys. Chem. B* **1999**, *103*, 9631.
(89) Tornblom, M.; Henriksson, U. *J. Phys. Chem. B* **1997**, *101*, 6028.
(90) Berr, S.; Jones, R. R. M.; Johnson, J. S. *J. Phys. Chem.* **1992**, *96*, 5611.
(91) Cang, H.; Fayer, M. D. *Dynamic Partitioning of an Aromatic Probe Between the Headgroup and Core Regions of Cationic Micelles*, submitted for publication.
(92) Romsted, L. S. Surfactants in Solution. In *Micellar Effects on Reaction Rates and Equalibria*; Lindman, B., Mittal, K. L., Eds.; Plenum Press: New York, 1984; Vol. 2; p 1015.
(93) Hirose, C.; Sepúlveda, L. *J. Phys. Chem.* **1981**, *85*, 3689.
(94) Tanford, C. *J. Phys. Chem.* **1972**, *76*, 3020.
(95) Berr, S. S. *J. Phys. Chem.* **1987**, *91*, 4760.
(96) Laaksonen, L.; Rosenholm, J. B. *Chem. Phys. Lett.* **1993**, *216*, 429.
(97) Vacatello, M.; Yoon, D. Y. *J. Chem. Phys.* **1990**, *92*, 757.
(98) Watanabe, K.; Ferrario, M.; Klein, M. L. *J. Phys. Chem.* **1988**, *92*, 819.
(99) Riddick, J. A.; Bunger, W. B. *Organic Solvents: Physical Properties and Methods of Purification*, 3rd ed.; John Wiley & Sons: New York, 1970; Vol. II.
(100) Zweig, A.; Maurer, A. H.; Roberts, B. G. *J. Org. Chem.* **1967**, *32*, 1322.
(101) Hall, L. R.; Iwamoto, R. T.; Hanzlik, R. P. *J. Org. Chem.* **1989**, *54*, 2446.
(102) Riddick, J. A.; Bunger, W. B.; Sakano, T. K. *Organic Solvents: Physical Properties and Methods of Purification*, 4th ed.; John Wiley & Sons: New York, 1986; Vol. II.
(103) Baur, J. E.; Wightman, R. M. *J. Electroanal. Chem.* **1991**, *305*, 73.
(104) Wightman, R. M.; Wipf, D. O. Ch. 3. In *Electroanalytical Chemistry*; Bard, A. J., Ed.; Marcel Dekker: New York, 1989; Vol. 15; Chapter 3.
(105) Peterson, K. A.; Stein, A. D.; Fayer, M. D. *Macromolecules* **1990**, *23*, 111.
(106) Atkins, P. W. *Physical Chemistry*, 4th ed.; W. H. Freeman and Company: New York, 1990.
(107) Moog, R. S.; Ediger, M. D.; Boxer, S. G.; Fayer, M. D. *J. Phys. Chem.* **1982**, *86*, 4694.
(108) Hu, C.-M.; Zwanzig, R. *J. Chem. Phys.* **1974**, *60*, 4354.
(109) Closs, G. L.; Miller, J. R. *Science* **1988**, *240*, 440.
(110) Guarr, T.; McLendon, G. *Coordination Chem. Rev.* **1985**, *68*, 1.
(111) Hale, J. M. The Rates of Reactions Involving Only Electron Transfer, at Metal Electrodes. In *Reactions of Molecules at Electrodes*; Hush, N. S., Ed.; Wiley-Interscience: New York, 1971; p 229.
(112) Liu, J. Y.; Bolton, J. R. *J. Phys. Chem.* **1992**, *96*, 1718.
(113) Markel, F.; Ferris, N. S.; Gould, I. R.; Myers, A. B. *J. Am. Chem. Soc.* **1992**, *114*, 6208.
(114) Chanon, M.; Hawley, M. D.; Fox, M. A. Introduction. In *Photoinduced Electron Transfer. Part A: Conceptual Basis*; Fox, M. A., Chanon, M., Eds.; Elsevier: New York, 1988; p 1.
(115) Miller, S. E.; Lukas, A. S.; Marsh, E.; Bushard, P.; Wasielewski, M. R. *J. Am. Chem. Soc.* **2000**, *122*, 7802.
(116) Nelsen, S. F.; Newton, M. D. *J. Phys. Chem. A* **2000**, *104*, 10023.
(117) Domingue, R. P.; Fayer, M. D. *J. Chem. Phys* **1985**, *83*, 2242.
(118) Burshtein, A. I. *Chem. Phys. Lett.* **1992**, *194*, 247.
(119) Burshtein, A. I.; Zharikov, A. A.; Shokhirev, N. V. *J. Chem. Phys.* **1992**, *96*, 1951.
(120) Burshtein, A. I.; Krissinel, E.; Mikhelashvili, M. S. *J. Phys. Chem.* **1994**, *98*, 7319.
(121) Os, N. M. v.; Haak, J. R.; Rupert, L. A. M. *Physico-Chemical Properties of Selected Anionic, Cationic, and Nonionic Surfactants*; Elsevier: Amsterdam, 1993.